

Simulation of a Particle Formation Stage in the Dispersion Polymerization of Styrene

Masahiro Yasuda,* Hidetoshi Seki, Hideki Yokoyama, Hiroyasu Ogino, Kosaku Ishimi, and Haruo Ishikawa

Department of Chemical Engineering, Osaka Prefecture University, 1-1 Gakuen-cho, Sakai, Osaka 599-8531, Japan

Received September 28, 2000; Revised Manuscript Received January 31, 2001

ABSTRACT: A model was proposed for simulation of a particle formation stage in the dispersion polymerization of styrene in ethanol. The role of poly(*N*-vinylpyrrolidone) molecules grafted by a polystyrene oligomer (PVP-*g*-PS) was taken into consideration for the particle stabilization. The model was derived based on the following mechanism: (i) polystyrene molecules whose degree of polymerization is greater than j_{cr} precipitate and form particles, (ii) particle aggregation due to the Brownian diffusion and the shear stress of the fluid continues until the amount of the PVP-*g*-PS molecules is enough to cover all the particle surface, and (iii) particles do not aggregate with each other once the entire particle surface is covered with the PVP-*g*-PS molecules. The theoretical particle concentrations calculated using the present model under various monomer concentrations and stirring speeds were in good agreement with the experimental data.

Introduction

Monodisperse polymer particles of micrometer size are used as standard particles for calibrating instruments, spacers of liquid-crystal panels, carrier particles for liquid chromatography columns, and particles for biomedical analyses.^{1,2} Monodisperse particles can be produced by the seeding method,³ the two-step swelling method,⁴ or dispersion polymerization.^{5,6}

Since monodisperse polymer particles whose diameter ranges from 1 to 20 μm can be synthesized in a single-step, many researchers are interested in dispersion polymerization. In dispersion polymerization, particles are formed in a reaction mixture which is initially homogeneous in the presence of a suitable steric stabilizer polymer. Styrene was polymerized in alcohol in the presence of a steric stabilizer such as hydroxypropyl cellulose or poly(*N*-vinylpyrrolidone) (PVP).^{5,7} When the polymerization conditions, such as temperature, stirring speed, solvent type, monomer composition and concentration, initiator type and concentration, and type and concentration of the steric stabilizer, are favorable, monodisperse particles can be obtained. To control the particle diameter and attain a narrow particle diameter distribution, several experimental studies concerning the effects of polymerization parameters were performed.^{5–15}

There are also several theoretical studies on the mechanism of dispersion polymerization. Teseng et al.⁵ described qualitatively the particle formation and growth in dispersion polymerization. According to them, the reaction mixture is homogeneous at the start of polymerization. When the reaction mixture is heated, free radicals are formed by initiator decomposition and grow in the continuous phase. Free radicals which attained a sufficiently high degree of polymerization precipitate and the stabilizer adsorb on the surface of the resulting particles to form stable particles. Once particles are formed, they absorb the monomer from the continuous

phase. After a sufficient number of particles which can capture free radicals in the continuous phase are formed, free radicals cannot grow to a sufficiently high degree of polymerization and polymerization mainly takes place within the monomer-swollen particles until all of the monomer is consumed.

Paine¹⁶ developed a multibin kinetic model for aggregation of precipitated radicals or unstabilized particles in dispersion polymerization. He assumed that the particle aggregation was controlled only by diffusion which was described by Smoluchowski¹⁷ and Frenklach¹⁸ and that the stabilized particles of which the surface was completely covered with poly(*N*-vinylpyrrolidone) molecules grafted by a polystyrene oligomer (PVP-*g*-PS) produced by the chain-transfer reaction of a radical with a stabilizer molecule do not aggregate with each other. According to the model, no new nuclei or particles are formed when particles are sufficiently stabilized. This was the first model that simulated quantitatively the role of the stabilizer molecules at the particle formation stage. However, this model still could not explain quantitatively the experimental results.

There are several other analyses concerning the kinetics of dispersion polymerization; however, there is no model that can theoretically simulate the whole mechanism of dispersion polymerization. This is because the particle formation mechanism of dispersion polymerization is too complicated. It is convenient to divide the whole process into two major stages, that is, an early stage (particle formation stage) in which the formation of particles or nuclei and aggregation between them are predominant and a later stage (particle growth stage) in which the particle growth is predominant. As a first step to develop a model which can simulate the whole process of dispersion polymerization, in a previous paper we proposed a simple model for the particle growth stage in dispersion polymerization.¹⁹ In this model, the experimental data obtained at the reaction time of 2 h were used as the initial values for the simulation. The theoretical time courses of the conversion and the particle diameter calculated using the model were in

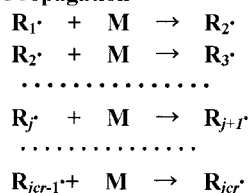
* Corresponding author. Telephone: +81-722-54-9299. Fax: +81-722-54-9911. E-mail: yasuda@chemeng.osakafu-u.ac.jp.

Polymerization in ethanol phase

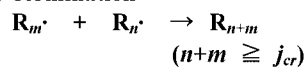
(1) Initiation



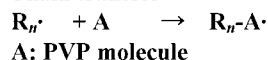
(2) Propagation



(3) Termination



(4) Chain transfer



Radical molecules in the ethanol phase are absorbed by the preexisted particles

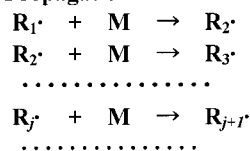
Precipitation

Polystyrene molecules whose degree of polymerization attained j_{cr} precipitate and form particles.

PVP-*g*-PS molecules in the ethanol phase adsorb on the particle surface

Polymerization in particles

(1) Propagation



(2) Termination



Stabilization

When all the particle surface is covered with PVP-*g*-PS molecules, the particle aggregation does not occur anymore.

Figure 1. Schematic illustration of particle formation stage in dispersion polymerization.

good agreement with the experimental data.

In the present paper, a model that can describe the behavior at the particle formation stage in dispersion polymerization was developed, and the predicted particle concentration was compared with the experimental results.

Theory

A Model at the Particle Formation Stage. The reaction scheme of polymerization in the ethanol phase and particles was assumed to be expressed by the well-established kinetics for radical polymerization.²⁰ To develop a quantitative model at the particle formation stage in dispersion polymerization, the mechanism of the particle formation in the dispersion polymerization of styrene was assumed, as shown in Figure 1. (a) Before heating, a styrene monomer, an initiator, and PVP exist in ethanol in a dissolved state. (b) When the reaction mixture is heated, the initiator molecules decompose and produce two initiator radicals per every initiator molecule. The initiator radicals react with the monomer and produce monomeric radicals. The monomeric radicals propagate by the chain reaction of the monomer and grow into oligomeric radicals. (c) The polystyrene molecules whose degree of polymerization attained j_{cr} precipitate and form nuclei or particles. These particles aggregate with each other by the Brownian diffusion and the shear stress of the fluid. (d) The PVP molecules produce the PVP-*g*-PS molecules. These molecules adsorb on the particle surface. When all the particle surface is covered with these molecules, the particle aggregation does not occur anymore. (e) Hereafter, particles grow by absorption of the oligomeric radicals from the ethanol phase and their polymerization within particles.

In addition to the particle formation mechanism mentioned above, the following assumptions were also made: (i) both the chain-transfer reactions in the ethanol phase and in particles can be neglected; (ii)

particle diameter distribution can be treated as monodisperse; (iii) the PVP-*g*-PS molecules produced in the ethanol phase adsorb promptly on the particle surface.

Polymerization in the Ethanol Phase. The reaction scheme of polymerization in the ethanol phase was described in Figure 1. The chain-transfer reactions in the ethanol phase were neglected because they were not significant compared with the other reactions in the dispersion polymerization of styrene.¹⁹ Furthermore, the disproportionation of the termination reaction was neglected because styrene was used as the monomer.²⁰

Particles can capture or absorb the radical molecules in the ethanol phase. When the particle diameter is quite small, the rate J_{R_j} of radical entry from the ethanol phase into particles is expressed by^{19,21,22}

$$J_{R_j} = 2\pi d_p N D_j [R_j] / V_{et} \quad (1)$$

where d_p is the mean particle diameter, N the total number of particles, D_j the diffusion coefficient of a radical molecule R_j whose degree of polymerization is j , $[R_j]$ the molar amount of a radical molecule R_j , and V_{et} the total volume of the ethanol phase. The diffusion coefficient D_j can be estimated using the following equation given by Lusis and Ratcliff:²³

$$D_j = \frac{(8.52 \times 10^{-21}) T}{\eta V_B} \left[1.40 \left(\frac{V_B}{j U_m} \right)^{1/3} + \left(\frac{V_B}{j U_m} \right) \right] \quad j = 1, 2, \dots, j_{cr} - 1 \quad (2)$$

η is the viscosity of ethanol, T the absolute temperature, U_m the molar volume of the monomer, and V_B the molar volume of ethanol.

Taking into account the capture of the radical molecules by particles and the three elementary reactions, that is, the initiation reaction of an initiator, the propagation reaction of the growing radicals, and the termination reaction between two radicals, the balance equations on each growing radical R_j in the ethanol

phase for a constant density batch reactor system are given as follows:

$$\frac{d[R_0]}{dt} = 2fk_d[I] - k_p \frac{[M_e]}{V_{et}} \frac{[R_0]}{V_{et}} V_{et} - k_t \frac{[R_0]}{V_{et}} \sum_{j=0}^{j_{cr}-1} \left(\frac{[R_j]}{V_{et}} \right) V_{et} - 2\pi d_p N D_0 \frac{[R_0]}{V_{et}} \quad (3)$$

$$\left. \begin{aligned} \frac{d[R_1]}{dt} &= k_p \frac{[M_e]}{V_{et}} \left(\frac{[R_0]}{V_{et}} - \frac{[R_1]}{V_{et}} \right) V_{et} - k_t \frac{[R_1]}{V_{et}} \sum_{i=0}^{j_{cr}-1} \left(\frac{[R_i]}{V_{et}} \right) V_{et} \\ &\quad - 2\pi d_p N D_1 \frac{[R_1]}{V_{et}} \\ &\vdots \\ \frac{d[R_j]}{dt} &= k_p \frac{[M_e]}{V_{et}} \left(\frac{[R_{j-1}]}{V_{et}} - \frac{[R_j]}{V_{et}} \right) V_{et} - k_t \frac{[R_j]}{V_{et}} \sum_{i=0}^{j_{cr}-1} \left(\frac{[R_i]}{V_{et}} \right) V_{et} \\ &\quad - 2\pi d_p N D_j \frac{[R_j]}{V_{et}} \\ &\vdots \\ \frac{d[R_{j_{cr}-1}]}{dt} &= k_p \frac{[M_e]}{V_{et}} \left(\frac{[R_{j_{cr}-2}]}{V_{et}} - \frac{[R_{j_{cr}-1}]}{V_{et}} \right) V_{et} - k_t \frac{[R_{j_{cr}-1}]}{V_{et}} \sum_{i=0}^{j_{cr}-1} \left(\frac{[R_i]}{V_{et}} \right) V_{et} \\ &\quad - 2\pi d_p N D_{j_{cr}-1} \frac{[R_{j_{cr}-1}]}{V_{et}} \end{aligned} \right\} \quad (4)$$

where f is the initiation efficiency, k_d the initiator decomposition rate constant in the ethanol phase, k_p the propagation rate constant in the ethanol phase, k_t the termination rate constant in the ethanol phase, $[I]$ the molar amount of initiator, and $[M_e]$ the molar amount of monomer in the ethanol phase. In eq 3, the degree of polymerization of the initiator radicals formed by the decomposition of the initiator was taken to be zero.

Formation and Aggregation of Particles. A polystyrene molecule whose degree of polymerization attained j_{cr} precipitates and forms a particle. The particles in the ethanol phase aggregate with each other by the Brownian diffusion and the shear stress of the fluid. The particle diameter distribution is probably wide at the early stage of particle formation. Therefore, in the modeling of the particle aggregation, various populations for particles from newly formed nuclei to particles containing a large number of radical molecules have to be taken into consideration. However, when the diameter distribution is wide, estimation of the aggregation rate is quite difficult. For example, for the aggregation caused by the Brownian diffusion, we must introduce the population balance equation of the particles with different particle diameters. Even with a modern computer, it is not easy to calculate simultaneously the particle aggregation and the radical polymerization in the ethanol phase and particles. Furthermore, for the aggregation caused by the shear stress of the fluid, we must introduce the aggregation coefficient on the basis of the orbital theory.²⁴ However, it is also not easy to estimate the Hamaker coefficient required for estimation of the aggregation coefficient. On the other hand, when the monodisperse particle diameter is assumed, we can use theoretically well-established equations for the particle aggregation.²⁵ Therefore, to simplify the particle aggregation and to minimize the number of parameters which must be established, we assumed that the particle size distribution is monodisperse.

The rate of decrease of the number N of monodisperse particles due to the aggregation by the Brownian diffusion is expressed by²⁵

$$N_B = - \frac{8k_B T}{3\mu} \left(\frac{N}{V_{et}} \right)^2 V_{et} \quad (5)$$

where k_B is the Boltzmann constant.

Using Smoluchowski's model concerning the particle motion in the fluid between two flat plates, the rate of decrease of the number N of monodisperse particles due to the aggregation by the shear stress of the fluid is expressed by²⁵

$$N_s = - \frac{4}{\pi} \tau \Phi_p \frac{N}{V_{et}} V_{et} \quad (6)$$

where τ is the shear speed and Φ_p the volume fraction of particles.

Metzner reported that the shear speed was proportional to the stirring speed n ²⁶

$$\tau = Kn \quad (7)$$

where K is a constant.

Therefore, taking into consideration both the aggregation due to the Brownian diffusion and the shear stress of the fluid, the change in the particle number N in the system is given by:

$$\begin{aligned} \frac{dN}{dt} &= \frac{k_t}{2} \sum_{k=1}^{j_{cr}-1} \left\{ \frac{[R_k]}{V_{et}} \sum_{i=1}^k \left(\frac{[R_{j_{cr}-i}]}{V_{et}} \right) \right\} V_{et} N_A + \\ &\quad k_p \frac{[M_e]}{V_{et}} \frac{[R_{j_{cr}-1}]}{V_{et}} V_{et} N_A - \frac{8k_B T}{3\mu} \left(\frac{N}{V_{et}} \right)^2 V_{et} - \\ &\quad \frac{4}{\pi} K n \Phi_p \frac{N}{V_{et}} V_{et} \quad (8) \end{aligned}$$

where N_A is Avogadro's number. The first and second terms of the right-hand side in eq 8 represent the new formation of polymer particles by the reaction and the others the decrease in the particle number due to the aggregation.

Polymerization in Particles. The total volume V_{pt} of polymer particles is related to the polymer volume V_{pp} , the monomer volume V_{pm} , and the ethanol volume V_{pe} in particles as follows:

$$V_{pt} = V_{pp} + V_{pm} + V_{pe} \quad (9)$$

V_{pm} and V_{pe} can be estimated using a thermodynamical model of the dispersion polymerization of styrene in ethanol.²⁷ In this thermodynamical model, the monomer concentration in particles was assumed to be in equilibrium with that in the ethanol phase. The total reaction volume V_t is related to V_{pt} and V_{et} by the following balance equation:

$$V_t = V_{pt} + V_{et} \quad (10)$$

The chain-transfer reactions in particles is not significant compared with the other reactions.¹⁹ The change in the polymer volume in a particle is caused by the propagation reaction in a particle and the entry of growing radicals into the particle. In general, the volume of a monomer unit in a polymer molecule in

particles can be equated to that of the monomer molecule in the ethanol phase. Therefore, the change in the total polymer volume V_{pp} in particles is given by

$$\frac{dV_{pp}}{dt} = \frac{k_t}{2} \sum_{k=1}^{j_{cr}-1} \left[\frac{[R_k]}{V_{et}} \sum_{i=1}^k \left\{ (j_{cr} - i + k) \frac{[R_{j_{cr}-i}]}{V_{et}} \right\} V_{et} \right] U_m + \left\{ 2\pi d_p N \sum_{k=1}^{j_{cr}-1} \left(k D_k \frac{[R_k]}{V_{et}} \right) \right\} U_m + k_p \frac{[M_e]}{V_{et}} \frac{[R_{j_{cr}-1}]}{V_{et}} V_{et} j_{cr} U_m + k_p \frac{[M_p]}{V_{pt}} \frac{N_R}{V_{pt}} V_{pt} U_m \quad (11)$$

where U_m is the molar volume of monomer, N_R the molar amount of the radical molecules in the total particles, and $[M_p]$ the molar amount of monomer in particles. The first and second terms of the right-hand side in eq 11 represent the volume change in the polymer molecules captured by particles. The third and the fourth terms represent the volume change due to new formation of polymer particles and the propagation in particles, respectively. The particle diameter d_p is calculated from V_{pt} as

$$d_p = \left(\frac{6 V_{pt}}{\pi N} \right)^{1/3} \quad (12)$$

The balance equation on the radical molecules in particles can be given by

$$\frac{dN_R}{dt} = 2\pi d_p N \sum_{k=0}^{j_{cr}-1} D_k \frac{[R_k]}{V_{et}} + k_p \frac{[M_e]}{V_{et}} \frac{[R_{j_{cr}-1}]}{V_{et}} V_{et} - k_t \left(\frac{N_R}{V_{pt}} \right)^2 V_{pt} \quad (13)$$

Monomer Concentration in the Ethanol Phase and Particles. The monomer is consumed by the propagation reaction in the ethanol phase and polymer particles. The consumption rate of monomer is given by

$$\frac{d[M_t]}{dt} = -k_p \frac{[M_e]}{V_{et}} \sum_{k=0}^{j_{cr}-1} \left(\frac{[R_k]}{V_{et}} \right) V_{et} - k_p \frac{[M_p]}{V_{pt}} \frac{N_R}{V_{pt}} V_{pt} \quad (14)$$

The total molar amount of monomer $[M_t]$ at time t is related to $[M_p]$ and $[M_e]$, the molar amount of monomer in particles and the ethanol phase, respectively, by the following mass balance equation:

$$[M_t] = [M_p] + [M_e] \quad (15)$$

The molar amount of monomer $[M_p]$ in particles can be estimated using the thermodynamical model of the dispersion polymerization of styrene in ethanol.²⁷

The conversion of monomer is defined by

$$X = ([M_t]_0 - [M_t])/[M_t]_0 \quad (16)$$

where $[M_t]_0$ is the total molar amount of monomer at the start of polymerization.

Stabilization of Particles. There are many studies concerning the stabilization mechanism of the particles in dispersion polymerization.^{3,12,16,28} Paine studied the

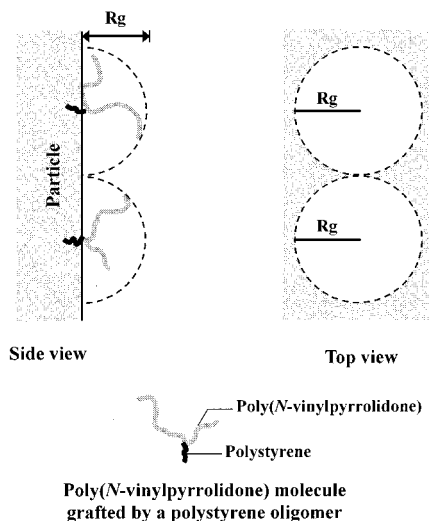


Figure 2. Schematic illustration of PVP-*g*-PS molecules adsorbed on particle surface.

particle stabilization mechanism only by the PVP-*g*-PS molecules.¹⁶ However, some researchers have reported that both the ungrafted PVP molecules and costabilizer play an important role in the formation of monodisperse polymer particles^{3,28} and others have reported that monodisperse polymer particles were obtained without the addition of a costabilizer.¹² As mentioned above, a consensus has not been obtained concerning the stabilization mechanism of the particles in dispersion polymerization. Therefore, the particle stabilization by the PVP-*g*-PS molecules proposed by Paine was adopted in the present model.

Paine¹⁶ assumed that the aggregation of particles ceases when all the particle surface is covered with the PVP-*g*-PS molecules, and thereafter particles grow by the capture of the growing radicals from the ethanol phase and polymerization in particles. The chain transfer reaction between the growing radical and PVP molecule in the ethanol phase produces a PVP-*g*-PS molecule. Paine¹⁶ predicted the amount of the PVP-*g*-PS produced in the ethanol phase, which was called "graft available", and the minimum amount of the PVP-*g*-PS required to prevent particle aggregation, which was called "graft required". The "graft available" is calculated by

$$\text{graft available} = C_s S N_A X \quad (17)$$

where C_s is the chain transfer coefficient of the polystyrene radicals against PVP and S the concentration of the monomer unit of PVP in the ethanol phase.

It is expected that the degree of the polymerization of polystyrene of the PVP-*g*-PS molecules affects their adsorption efficiency. However, it is difficult to estimate the adsorption efficiency of the PVP-*g*-PS molecules at this stage. Therefore, an ideal situation in which all of the produced PVP-*g*-PS molecules adsorb on the particle surface was assumed in the present simulation.

Figure 2 shows schematically the PVP-*g*-PS molecules adsorbed on the particle surface. Paine calculated the minimum amount of the PVP-*g*-PS molecules required to stabilize the particles against the aggregation.¹⁶ Therefore, using a method similar to Paine, the minimum amount of the PVP-*g*-PS molecules was calculated. The radius R_g of gyration of a PVP molecular chain in the ethanol phase can be calculated by AM_{m-PVP}^b where

A and b are constants and M_{m-PVP} is the molecular mass of a PVP molecule. To estimate R_g of the PVP- g -PS, the average length of the long chain from the grafting point is needed. The average length of the long chain from the grafting point was assumed to be 75% of that of PVP. Therefore, the coverage area Q of a PVP- g -PS molecule is given by:

$$Q = \pi R_g^2 = \pi A^2 (0.75 M_{m-PVP})^{2b} \quad (18)$$

Using the relation of eq 18, the "graft required" is given by

$$\text{graft required} = (N\pi d_p^2)/Q = \frac{Nd_p^2}{A^2 (0.75 M_{m-PVP})^{2b}} \quad (19)$$

As mentioned above, a prompt adsorption of the PVP- g -PS molecules on the particle surface was assumed. Therefore, when the value of the graft available attains that of the graft required, all the particle surface is covered with PVP- g -PS molecules and particle aggregation stops occurring. This time is defined as t_{stb} .

Experimental Section

Materials. Styrene and 2,2'-azobisisobutyronitrile (AIBN) were purchased from Wako Pure Chemicals Co. Ltd. (Osaka, Japan). Styrene was washed with a 10% sodium hydroxide solution and passed through a column packed with activated aluminum oxide to remove an inhibitor before use. AIBN was recrystallized twice in methanol. PVP with a nominal molecular mass of 40 000, cetyl alcohol, ethanol, hydroquinone, and tetrahydrofuran (THF) were purchased from Nacalai Tesque (Kyoto, Japan). These reagents were used without purification.

Counting of the Particle Number. The particle number was counted using a Burkert Turk hemacytometer (Elma, Tokyo, Japan).

Synthesis of Particles. To compare with the theoretical particle concentration calculated using the above model, the dispersion polymerization of styrene in ethanol was performed in a glass batch reactor equipped with a motor-driven Teflon stirrer. Figure 3 schematically shows the reactor setup and the stirrer. The compositions of the reaction mixtures are shown in Table 1. A clean and dry 300 mL separable-flask was charged with ethanol, PVP, and cetyl alcohol and then covered with a four-neck separable-cover attached to a Dimroth condenser. The flask was heated to 70 °C under agitation at 30 rpm for 20 min. AIBN was weighed into styrene and the resulting solution was quickly poured into the flask. The reactions were run for 24 h with agitation at various stirring speed. Then, the flask was cooled in an iced-water bath and the reaction mixture was transferred to four 50 mL test tubes. The particles formed were washed by repeating centrifugal separation and suspension in ethanol and distilled water.

Estimation of j_{cr} . To estimate the critical degree of polymerization j_{cr} of which a radical molecule precipitates in the ethanol phase and forms a particle, the molecular mass distribution of polymers in the ethanol phase at a reaction time of 1 h was measured. The preparation of the reaction mixture, the reaction equipment, and the procedure at the beginning of the reaction were the same as in the synthesis of particles. The reactions were proceeded for 1 h under agitation. Then, to stop polymerization 1 g of hydroquinone was added to the flask. The reaction mixture was transferred to four 50 mL test tubes, and the particles in the reaction mixture were removed by centrifugation. A small portion of the supernatant was added to 500 mL of methanol and the precipitated polymer was collected. The molecular mass distribution of the polymer was measured using a Shimadzu liquid chromatograph LC-5A (Shimadzu, Kyoto, Japan) with a Wakobeads G-40 column (Wako; 7.8 mm in diameter and 300 mm in length) using THF as a carrier liquid ($8.3 \times 10^{-9} \text{ m}^3 \cdot \text{s}^{-1}$). A Shimadzu SPD-2A

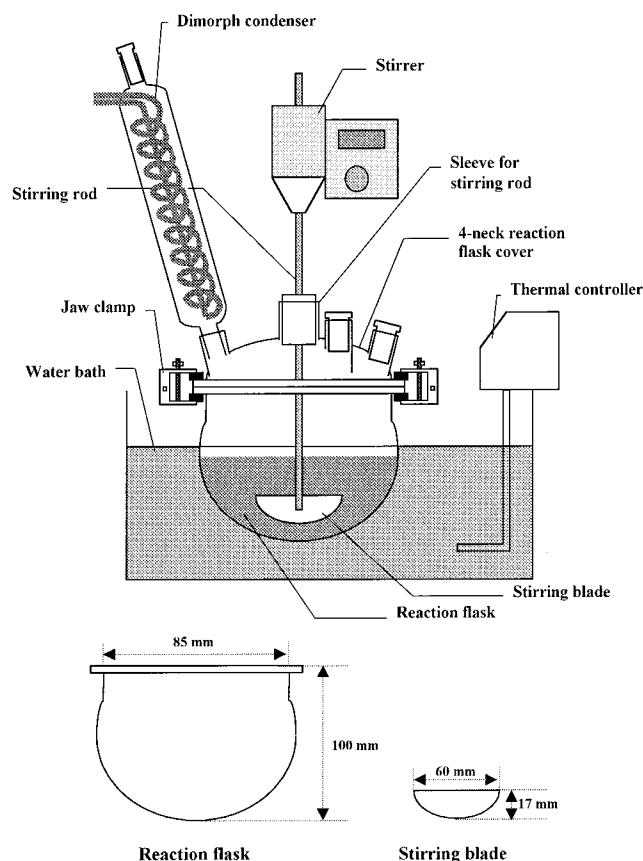


Figure 3. Experimental equipment of dispersion polymerization.

Table 1. Composition of Reaction Mixtures^a

component (wt %)	run				
	1	2	3	4	5
ethanol	67.40	72.50	77.50	82.55	87.60
PVP	1.80	1.80	1.80	1.80	1.80
cetyl alcohol	0.50	0.50	0.50	0.50	0.50
styrene	30.0	25.0	20.0	15.0	10.0
2,2'-azobisisobutyronitrile	0.30	0.25	0.20	0.15	0.10

^a Total amount: 100 g.

UV detector was calibrated at 265 nm using the polystyrene molecular mass standards from GL-Science (Tokyo, Japan) and then used to measure the polymer concentration.

Results and Discussion

Simulation of Particle Formation. To simulate the particle formation and the particle aggregation at the particle formation stage of dispersion polymerization, the differential equations, eqs 3, 4, 8, 11, 13, and 14, were solved numerically using the Runge-Kutta-Gill method under the following initial conditions:

$$t = 0; \quad [R_j] = 0 \quad (j = 1, \dots, j_{cr} - 1), \quad N = 0, \\ V_{pp} = 0, \quad N_R = 0, \quad [M_i] = [M_i]_0 \quad (20)$$

The rate constants k_d , k_t , and k_p at 70 °C were obtained from literature.²⁹ The value of the initiator efficiency f was also taken from literature.³⁰ The rate constants used in the calculation are listed in Table 2. The propagation rate constant was taken to be independent of the phase.

Table 3 shows the K values for various impeller types.²⁶ In the present simulation, a value of 13.0 for a

Table 2. Rate Constants Used in the Calculation

$$\begin{aligned}
 k_d &= 3.77 \times 10^{-5} \text{ s}^{-1} \\
 k_p &= 3.52 \times 10^{-1} \text{ m}^3 \cdot \text{mol}^{-1} \cdot \text{s}^{-1} \\
 k_t &= 6.10 \times 10^4 \text{ m}^3 \cdot \text{mol}^{-1} \cdot \text{s}^{-1} \\
 f &= 0.58
 \end{aligned}$$

Table 3. *K* Values for Various Impellers

impeller type	<i>K</i> value (N·s·m ⁻²)
flat blade turbine	11.5 ± 1.4
fan blade turbine	13.0 ± 2.0
marine propeller	10.0 ± 0.9

Table 4. Various Parameters Used in the Calculation

<i>U_m</i>	1.33 × 10 ⁻⁴ m ³ ·mol ⁻¹
<i>j_{cr}</i>	120
<i>K</i>	13.0
<i>n</i>	0.5–2.0 s ⁻¹ (30–120 rpm)
<i>V_t</i>	1.22 × 10 ⁻⁴ m ³
[<i>M_t</i>] ₀	9.60 × 10 ⁻² to 2.88 × 10 ⁻¹ mol
[<i>I</i>] ₀	6.09 × 10 ⁻⁴ to 1.82 × 10 ⁻³ mol
<i>C_s</i>	1.0 × 10 ⁻⁴
<i>S</i>	1.33 × 10 ² mol·m ⁻³
<i>R_g</i>	1.4 × 10 ⁻⁸ m
<i>A</i>	5.3 × 10 ⁻⁷ m·mol·kg ⁻¹
<i>b</i>	0.32

flat blade turbine was used as the *K* value. The chain transfer constant *C_s*, the *R_g* value, and the constant and exponent in eq 18 were obtained from the literature.¹⁶

The critical degree of polymerization *j_{cr}* was estimated by measuring the molecular masses of the polymers in the ethanol phase at a reaction time of 1 h. This measurement was based on the assumption that the polymer molecules having the highest degree of the polymerization in the ethanol phase at the reaction time of 1 h was the same as that at the particle formation step. The highest degree of polymerization in the ethanol phase was 120 when the monomer concentration and the stirring speed were 20 wt % and 30 rpm, respectively. This value was not so different from the values measured under the other monomer concentration and the stirring speed conditions. Therefore, 120 was used as the *j_{cr}* value irrespective of the monomer concentration and the stirring speed.

U_m was estimated by the method of Le Bas.³¹ Other various parameters used in the calculation are listed in Table 4 together with the values mentioned above.

In the present model, particles do not aggregate with each other after *t_{stb}* when the PVP-*g*-PS molecules cover all the particle surface. To estimate *t_{stb}*, the graft required and the graft available were calculated. Figure 4 compares the time course of the graft required with that of the graft available when the monomer concentration and stirring speed were 20 wt % and 30 rpm, respectively. As can be seen in the figure, the graft available was greater than the graft required when time is greater than 356 s (= *t_{stb}*). The calculated particle diameter, the conversion and the particle concentration at *t_{stb}* were 2.48 × 10⁻⁷ m, 6.05 × 10⁻²%, and 2.03 × 10¹⁶ m⁻³, respectively. The calculated particle diameter and the conversion were slightly greater than those estimated by Paine.¹⁶ This difference may be attributed to the fact that Paine did not take into consideration the aggregation due to the shear stress of the fluid.

When the production rate of the PVP-*g*-PS molecules in the ethanol phase calculated by eq 17 and the diffusion rate of the PVP-*g*-PS molecules to the particle surface calculated by eq 1 were compared, the latter was about 4000-fold faster than the former. Therefore, it is reasonable to assume that the PVP-*g*-PS molecules

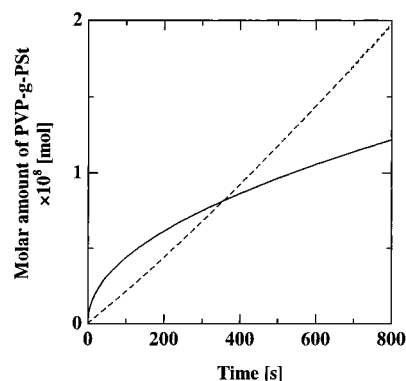


Figure 4. Time courses of the molar amount of PVP-*g*-PS produced and the molar amount of PVP-*g*-PS required for particle stabilization. Broken line shows the PVP-*g*-PS produced and solid line the PVP-*g*-PS required for particle stabilization. Monomer concentration and stirring speed are 20 wt % and 30 rpm, respectively.

produced in the ethanol phase adsorb promptly on the particle surface.

The particle formation stage terminates at *t_{stb}* and is followed by the particle growth stage. After *t_{stb}*, the above basic differential equations can be used to simulate the particle growth stage by taking *d(N)/dt* = 0 in eq 8. However, in the present calculations, the termination rate constant in particles at the particle formation stage was regarded to be equivalent to that in the ethanol phase while at the particle growth stage it was regarded to be about 1/130th of that in the ethanol phase. Therefore, to simulate the whole process in dispersion polymerization, the termination rate constant in particles should be studied. However, it is not easy to estimate the termination rate constant in particles. To study the effect of the termination in particles on the particle concentration and the particle diameter, a simulation in which the termination rate constant in particles was taken to be 1/130th of that of the ethanol phase was performed under the same monomer concentration (20 wt %) and the stirring speed (30 rpm) described above. The calculated particle diameter was 2.43 × 10⁻⁷ m, which was 98% of that described above (2.48 × 10⁻⁷ m). The calculated particle concentration agreed with the value described above (2.03 × 10¹⁶ m⁻³). These results indicate that the effect of the termination rate constant in particles on the particle concentration and the particle diameter is negligible at the particle formation stage. According to the discussion of the termination in particles in the present study, the termination rate constant in particles can be taken to be 1/130th of that of the ethanol phase. However, to estimate the precise termination rate constant in particles at the particle formation stage, further study is needed in the future.

Effect of the Monomer Concentration on Particle Formation. The monomer concentration affects the particle formation rate. Therefore, the effect of the monomer concentration on the particle formation in dispersion polymerization was first studied. Figure 5 shows the time courses of the conversion under various monomer concentrations. The calculations were stopped when time *t* attained *t_{stb}*. When the monomer concentration was high, the total polymerization rate was high, which was calculated from the sum of the polymerization rate in particles and that in the ethanol phase. Figures 6 and 7 show the time courses of the particle diameter and the number of radical molecules in a

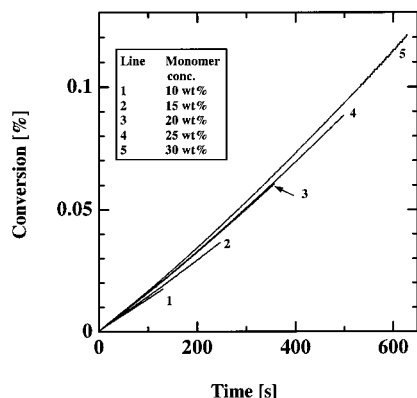


Figure 5. Time courses of conversion at 30 rpm under various monomer concentrations.

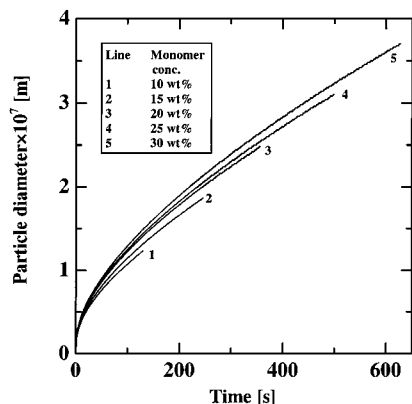


Figure 6. Time courses of the particle diameter at 30 rpm under various monomer concentrations.

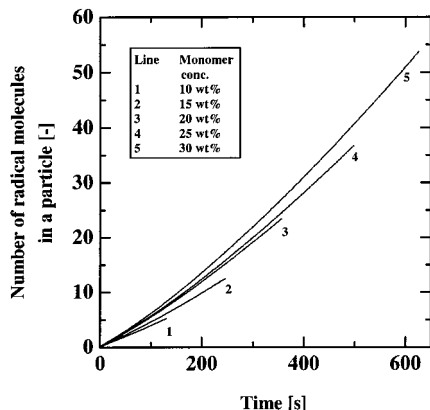


Figure 7. Time courses of the number of radical molecules in a particle at 30 rpm under various monomer concentrations.

particle under various monomer concentrations. The particle diameter and the number of radical molecules in a particle were high when the monomer concentration was high. Furthermore, the higher the monomer concentration was, the higher the total concentration of the radical molecules in the ethanol phase was (data were not shown). These results suggested that both the polymerization rates in the ethanol phase and particles were high when the monomer concentration was high.

In the present model, the particle aggregation due to the Brownian diffusion and the shear stress of the fluid were both taken into consideration. Figure 8 shows the time courses of the rate of the particle aggregation due to the Brownian diffusion. The rate of the particle aggregation due to the Brownian diffusion rapidly decreased with time, in accordance with eq 5 in which

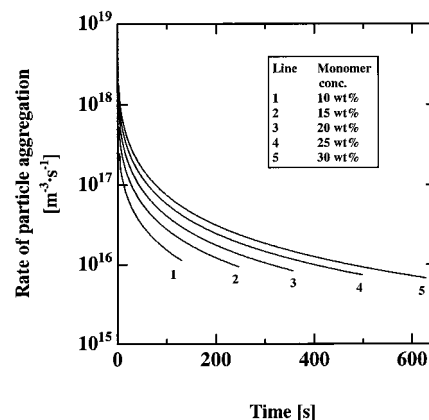


Figure 8. Rate of particle aggregation due to the Brownian diffusion at 30 rpm under various monomer concentrations.

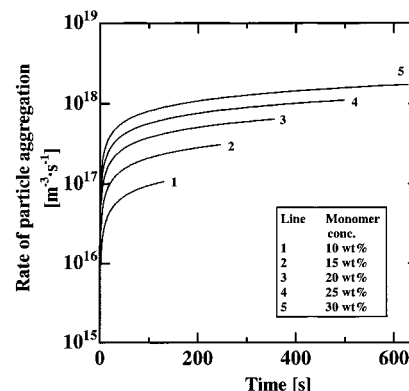


Figure 9. Rate of particle aggregation due to the shear stress of the fluid at 30 rpm under various monomer concentrations.

the particle aggregation caused by the Brownian diffusion is proportional to the square of the particle concentration N . Figure 9 shows the time courses of the rate of the particle aggregation due to the shear stress of the fluid. The rate of the particle aggregation due to the shear stress rapidly increased with time and then became almost constant. This is interpreted by eq 6 in which the particle aggregation due to the shear stress of the fluid is proportional to the particle concentration N and the volume fraction Φ_p of particles. Although the particle concentration decreases with the time, the volume fraction of particles formed by precipitation of the radicals whose degree of polymerization attained j_{cr} increases. From Figures 8 and 9, at the very early stage of the reaction when many particles exist in the ethanol phase, the particle aggregation is mainly caused by the Brownian diffusion, and that due to the shear stress of the fluid soon becomes predominant. In the case of a monomer concentration of 10 wt %, the rate of the particle aggregation due to the shear stress of the fluid at about 30 s exceeds that due to the Brownian diffusion. In the other monomer concentrations, the time when the rate of the particle aggregation due to the shear stress of the fluid exceeds that due to the Brownian diffusion was shorter than that of 10 wt %.

As shown above, the particle aggregation due to the shear stress of the fluid plays an important role in the particle formation stage in dispersion polymerization. However, Paine¹⁶ did not take into consideration the particles aggregation due to the shear stress of the fluid.

Figure 10 shows the time courses of the particle concentration. The particle concentration decreased with time until t_{stb} and hereafter became constant as

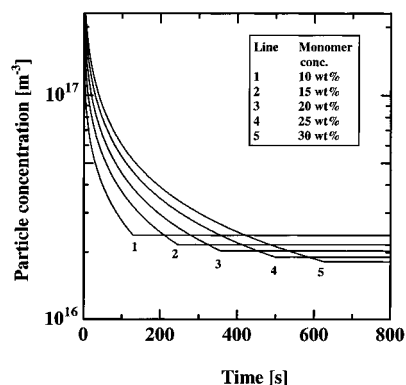


Figure 10. Time courses of particle concentration at 30 rpm under various monomer concentrations.

Table 5. Effect of Monomer Concentration on t_{stb} Value and Particle Concentration, Particle Diameter, and Conversion at t_{stb}

monomer concn (wt %)	t_{stb} (s)	particle concn (m^{-3})	particle diam (m)	convn (%)
10	130	2.38×10^{16}	1.23×10^{-7}	1.75×10^{-2}
15	246	2.16×10^{16}	1.87×10^{-7}	3.65×10^{-2}
20	356	2.03×10^{16}	2.48×10^{-7}	6.05×10^{-2}
25	498	1.90×10^{16}	3.10×10^{-7}	8.84×10^{-2}
30	628	1.81×10^{16}	3.70×10^{-7}	1.21×10^{-1}

assumed above. The higher the monomer concentration was, the slower their decrease was until t_{stb} . This is because the formation rate of particles is higher when the monomer concentration is higher.

Table 5 summarizes the t_{stb} value, the particle concentration, the particle diameter, and the conversion at t_{stb} under various monomer concentration conditions. The higher the monomer concentration was, the longer t_{stb} was. The polymerization rate in the ethanol phase was high when the monomer concentration was high as described above. The high polymerization rate in the ethanol phase resulted in the high production rate of the PVP-*g*-PS molecules. However, the total surface area of particles which had to be covered with the PVP-*g*-PS molecules increased simultaneously with increase in the particle concentration. The increase in the graft required at the beginning of the reaction was greater than that in the graft available when the monomer concentration was high (data were not shown). Therefore, t_{stb} was prolonged under the high monomer concentration.

Effect of Stirring Speed on Particle Formation.

The effect of the stirring speed on the particle formation was studied. Figure 11 shows the time courses of the rate of the particle aggregation due to the shear stress of the fluid. When the stirring speed was high, the rate of the particle aggregation due to the shear stress of the fluid was high.

Figure 12 shows the time courses of the conversion at various stirring speeds. When the stirring speed was high, the rate of polymerization was high. In the solution polymerization in which all the components of the reaction mixture exist in solvent in a dissolved state, there is no effect of stirring speed on the polymerization rate. The calculation results shown in Figure 12 indicated that the existence of particles affected the polymerization rate.

To clarify why the polymerization rate at a high stirring speed was higher than that at a low stirring speed, the effect of the stirring speed on the mass transfer rates of radicals and monomer and the polymerization rate were studied. Table 6 compares the

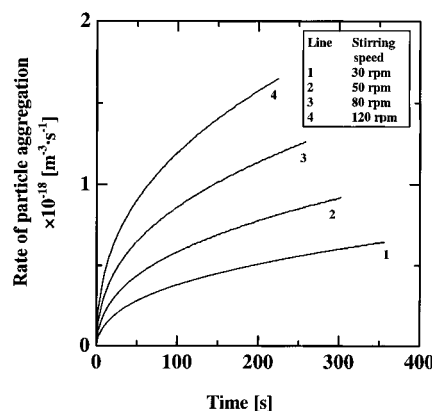


Figure 11. Time courses of rate of particle aggregation due to the shear stress of the fluid at a monomer concentration of 20 wt % under various stirring speeds.

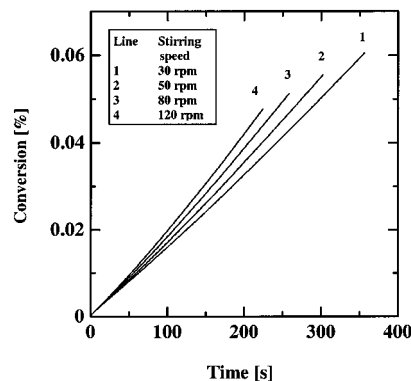


Figure 12. Time courses of the conversion at a monomer concentration of 20 wt % under various stirring speeds.

various particle properties, the mass transfer rates of radicals and monomer, and the polymerization rates at 30 and 120 rpm at the reaction time of 100 s. When the polymerization rates in the ethanol phase were compared with those in particles at two stirring speeds, the rates in the ethanol phase were both about 30–40-fold greater than those in particles. This result indicates that the polymerization mainly takes place in the ethanol phase. This was because the high monomer concentration in the ethanol phase at the high stirring speed was caused by the slightly low radical absorption rate from the ethanol phase to particles. In the case of emulsion polymerization,³² the decrease in the total particle surface area was expected to result in the high radical absorption rate from the ethanol phase to particles. However, in dispersion polymerization the simulation result was reverse, that is, the radical absorption rate at 120 rpm was lower than that at 30 rpm. The discrepancy was probably caused by the facts that the particle diameter in emulsion polymerization was 10–100-fold smaller than that in dispersion polymerization and the particle number in emulsion polymerization was 100–1000-fold greater than that in dispersion polymerization.

Table 7 summarizes the effect of the stirring speed on the t_{stb} value, the particle concentration, the particle diameter, and the conversion at t_{stb} . The higher the stirring speed was, the shorter t_{stb} was. The high stirring speed resulted in the high rate of particle aggregation due to the shear stress of the fluid and the low surface area which had to be stabilized by the PVP-*g*-PS molecules as described above. Therefore, the t_{stb} value was short when the stirring speed was high.

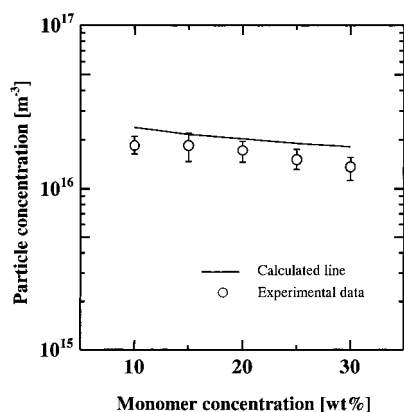
Table 6. Effect of Stirring Speed on Particle Properties, Mass Transfer Rates of Radicals and Monomer, and Polymerization Rates at 100 s^a

	stirring speed	
	30 rpm	120 rpm
particle concn (m ⁻³)	3.74×10^{16}	2.45×10^{16}
particle diam (m)	1.22×10^{-7}	1.50×10^{-7}
tot. particle surface area ^b (m ²)	1.76×10^3	1.73×10^3
tot. particle vol ^b (m ³)	3.59×10^{-5}	4.30×10^{-5}
radical concn in particles (mol·m ⁻³)	9.54×10^{-3}	8.63×10^{-3}
radical abs rate ^b from ethanol phase to particles (mol·s ⁻¹)	4.26×10^{-4}	4.22×10^{-4}
radical concn in ethanol phase (mol·m ⁻³)	8.90×10^{-6}	1.18×10^{-5}
monomer concn in particles (mol·m ⁻³)	1.33×10^3	1.33×10^3
monomer concn in ethanol phase (mol·m ⁻³)	1.60×10^3	1.60×10^3
polymerization rate ^b in particles (mol·s ⁻¹)	1.38×10^{-4}	1.49×10^{-4}
polymerization rate ^b in ethanol phase (mol·s ⁻¹)	4.30×10^{-3}	5.70×10^{-3}

^a Radical absorption rate was calculated by eq 1 ($2\pi d_p N(\Sigma D_i [R_i]) / V_{et}$). Polymerization rates (monomer consumption rate) were calculated by $k_p [M] \Sigma [R_i] / V_{et}$. ^b Per 1 m³ of the reaction mixture.

Table 7. Effect of Stirring Speed on t_{stb} Value and Particle Concentration, Particle Diameter, and Conversion at t_{stb}

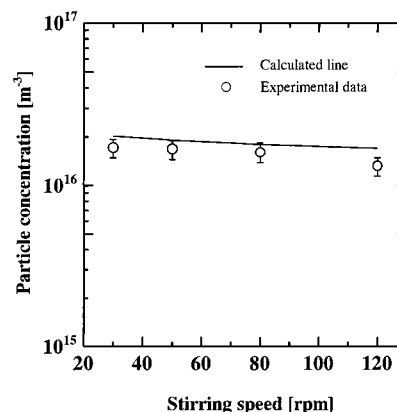
stirring speed (rpm)	t_{stb} (s)	particle concn (m ⁻³)	particle diam (m)	convn (%)
30	356	2.03×10^{16}	2.48×10^{-7}	6.05×10^{-2}
50	302	1.91×10^{16}	2.44×10^{-7}	5.55×10^{-2}
80	258	1.80×10^{16}	2.42×10^{-7}	5.12×10^{-2}
120	224	1.70×10^{16}	2.40×10^{-7}	4.77×10^{-2}

**Figure 13.** Comparison of the theoretical predictions of the particle concentration at 30 rpm under various monomer concentrations with the experimental data.

Comparison of the Theoretical Prediction with the Experimental Data. To test the validity of the present model, experiments of the dispersion polymerization of styrene in ethanol were performed in an isothermal batch reactor. It was difficult to measure exactly the particle concentration at t_{stb} . Using the multibin kinetic model, Paine¹⁶ proved that the monodispersity of particles was lost when particle aggregation occurred after t_{stb} . Furthermore, the total particle concentrations at the reaction times from 2 to 24 h were constant.¹⁹ Therefore, the particle concentration at a reaction time of 24 h was used as the experimental value at t_{stb} .

Figure 13 compares the theoretical predictions of the particle concentration under various monomer concentrations with the experimental data. The theoretical line calculated using the present model was in good agreement with the experimental data.

Figure 14 compares the theoretical predictions of the particle concentration under various stirring speeds with the experimental data. The theoretical line calculated using the present model was also in good agreement with the experimental data.

**Figure 14.** Comparison of the theoretical predictions of the particle concentration at a monomer concentration of 20 wt % under various stirring speeds with the experimental data.

As shown in Figures 13 and 14, the theoretical prediction of the particle concentration at time t_{stb} under various monomer concentrations and stirring speeds agreed well with the experimental results measured at the time 24 h, indicating that the model can simulate quantitatively the particle formation stage in dispersion polymerization.

Conclusion

A model was proposed for simulating the particle formation stage in the dispersion polymerization of styrene based on several assumptions. In the model, the polymerization reactions in the ethanol phase and the particle aggregation due to the shear stress of the fluid, which was neglected by previous investigator,^{5,16,33} in addition to that due to the Brownian diffusion were taken into consideration. The theoretical calculations showed that the aggregation caused by the shear stress of the fluid played an important role in the particle formation stage in dispersion polymerization. The theoretical predictions of the particle concentration under various monomer concentrations and stirring speeds agreed well with the experimental data, indicating that the model can simulate quantitatively the particle formation stage in dispersion polymerization.

The calculated results, such as the t_{stb} value, the conversion, the particle diameter, the number of radical molecules in a particle, and the particle concentration at t_{stb} , can be used as the initial conditions to solve the basic differential equations of the model¹⁹ for the particle growth stage of dispersion polymerization. However, in the present calculation the termination rate

constant in particles at the particle formation stage was regarded to be equivalent to that in the ethanol phase while in the particle growth stage it was regarded to be about $1/130$ th of that in the ethanol phase. Therefore, to simulate quantitatively the whole process in dispersion polymerization, the termination rate constant in particles should be studied.

Nomenclature

A , constant ($\text{m}\cdot\text{mol}\cdot\text{kg}^{-1}$)

b , exponent

C_s , chain transfer coefficient of polystyrene radical against PVP

D_j , diffusion coefficient of a radical whose degree of polymerization is j in the ethanol phase ($\text{m}^2\cdot\text{s}^{-1}$)

d_p , particle diameter (m)

f , initiation efficiency

$[I]$, molar amount of initiator in the ethanol phase (mol)

$[I]_0$, initial molar amount of initiator in the ethanol phase (mol)

J_{R_p} , rate of radical entry into polymer particles ($\text{mol}\cdot\text{s}^{-1}$)

j_{cr} , critical degree of polymerization of radicals in the ethanol phase

K , constant in eq 7 ($\text{N}\cdot\text{s}\cdot\text{m}^{-2}$)

k_B , Boltzmann constant ($\text{J}\cdot\text{K}^{-1}$)

k_d , decomposition rate constant of initiator (s^{-1})

k_p , propagation rate constant ($\text{m}^3\cdot\text{mol}^{-1}\cdot\text{s}^{-1}$)

k_t , termination rate constant in the ethanol phase ($\text{m}^3\cdot\text{mol}^{-1}\cdot\text{s}^{-1}$)

$[M_e]$, molar amount of monomer in the ethanol phase (mol)

$[M_p]$, molar amount of monomer in particles (mol)

$[M_t]$, total molar amount of monomer (mol)

$[M_t]_0$, initial total molar amount of monomer (mol)

M_{m-PVP} , average molecular mass of PVP

n , stirring speed (s^{-1})

N , total number of polymer particles

N_A , Avogadro's number (mol^{-1})

N_B , rate of decrease of the number of particles due to the aggregation by the Brownian diffusion (s^{-1})

N_R , molar amount of radical molecules in total particles (mol)

N_S , rate of decrease of the number of particles due to the aggregation by the shear stress of the fluid (s^{-1})

Q , coverage area a PVP- g -PS molecule on particle (m^2)

R_g , radius of gyration of a PVP chain in the ethanol phase (m)

R_j , radical whose degree of polymerization is j

$[R_j]$, molar amount of radical R_j (mol)

S , concentration of monomer unit of PVP in the ethanol phase ($\text{mol}\cdot\text{m}^{-3}$), * PVP monomer unit

T , temperature (K)

t , reaction time (s)

t_{stb} , time required to stabilize particles or the time when the graft available attains the graft required (s)

U_m , molar volume of repeating unit in a polymer chain ($\text{m}^3\cdot\text{mol}^{-1}$)

V_B , molar volume of ethanol ($\text{m}^3\cdot\text{mol}^{-1}$)

V_{et} , total volume of the ethanol phase (m^3)

V_{pt} , total particle volume (m^3)

V_{pe} , ethanol volume in particles (m^3)

V_{pm} , monomer volume in particles (m^3)

V_{pp} , polymer volume in particles (m^3)

V_t , total reaction volume (m^3)

X , conversion

Φ_p , volume fraction of particles

η , viscosity of ethanol ($\text{Pa}\cdot\text{s}$)

τ , shear speed ($\text{N}\cdot\text{m}^{-2}$)

References and Notes

- (1) Ugelstad, J.; Söderberg, L.; Berge, A.; Bergström, J. *Nature* **1983**, *303*, 95–98.
- (2) Ugelstad, J.; Mørk, P. C.; Berge, A.; Ellingsen, T.; Khan, A. A. In *Emulsion polymerization*; Piirma, I., Ed.; Academic Press: New York, 1982; Chapter 11, pp 383–413.
- (3) Vanderhoff, J. W.; El-Aasser, M. S.; Mical, F. J.; Sudol, E. D.; Teseng, C. M.; Silwanowicz, A.; Kornfeld, D. M.; Vincente, F. A. *J. Dispers. Sci. Technol.* **1984**, *5*, 231–246.
- (4) Ugelstad, J.; Mørk, P. C.; Kaggerud, K. H.; Ellingsen, T.; Berge, A. *Adv. Colloid Interface Sci.* **1980**, *13*, 101–140.
- (5) Teseng, C. M.; Lu, Y. Y.; El-Aasser, M. S.; Vanderhoff, J. W. *J. Polym. Sci., Part A* **1988**, *24*, 2995–3007.
- (6) Almog, Y.; Reich, S.; Levy, M. *Br. Polym. J.* **1982**, *14*, 131–136.
- (7) Ober, C. K.; Lok, K. P.; Hair, M. L. *J. Polym. Sci. Polym. Lett. Ed.* **1985**, *23*, 103–108.
- (8) Sáenz, J. M.; Asua, J. M. *J. Polym. Sci., Part A* **1995**, *33*, 1511–1521.
- (9) Desmazes, P. L.; Guillot, J. *J. Polym. Sci., Part A* **1998**, *36*, 325–335.
- (10) Paine, A. J. *Macromolecules* **1990**, *23*, 3104–3109.
- (11) Chen, Y.; Yang, H. W. *J. Polym. Sci., Part A* **1992**, *30*, 2765–2772.
- (12) Paine, A. J.; McNulty, J. *J. Polym. Sci., Part A* **1990**, *28*, 2569–2574.
- (13) Paine, A. J. *J. Polym. Sci., Part A* **1990**, *28*, 2485–2500.
- (14) Lok, K. P.; Ober, C. K. *Can. J. Chem.* **1985**, *63*, 209–216.
- (15) Ober, C. K.; Lok, K. P. *Macromolecules* **1987**, *20*, 268–273.
- (16) Paine, A. J. *Macromolecules* **1990**, *23*, 3109–3117.
- (17) Smoluchowski, M. V. *Z. Phys. Chem.* **1917**, *192*, 129–168.
- (18) Frenklach, M. *J. Colloid Interface Sci.* **1985**, *108*, 237–242.
- (19) Yasuda, M.; Yokoyama, H.; Seki, H.; Ogino, H.; Ishimi, K.; Ishikawa, H. *Macromol. Theory Simul.* **2001**, *10*, 54–62.
- (20) Flory, P. J. *Principles of Polymer Chemistry*; Cornell University Press: New York, 1953; Chapter 4, pp 106–177.
- (21) Gilbert, R. G. *Emulsion Polymerization*; Academic Press: New York, 1995; Chapter 2, pp 24–77.
- (22) Nomura, M. In *Emulsion Polymerization*; Piirma, I., Ed.; Academic Press: New York, 1982; Chapter 5, pp 191–219.
- (23) Lusi, M. A.; Ratcliff, G. A. *Can. J. Chem. Eng.* **1968**, *46*, 385–386.
- (24) Batchelor, G. K.; Green, J. T. *J. Fluid Mech* **1972**, *56*, 375–383.
- (25) Swift, D. L.; Friedlander, S. K. *J. Colloid Sci.* **1964**, *19*, 621–647.
- (26) Metzner, A. B. *AIChE J.* **1961**, *7*, 3–15.
- (27) Lu, Y. Y.; El-Aasser, M. S.; Vanderhoff, J. W. *J. Polym. Sci., Part B* **1988**, *26*, 1187–1203.
- (28) Shen, S.; Sudol, E. D.; El-Aasser, M. S. *J. Polym. Sci., Part A* **1990**, *32*, 1087–1100.
- (29) Brandrup, J.; Immergut, E. H., Eds. *Polymer Handbook*, 3rd ed.; Wiley-Interscience: New York, 1989.
- (30) Ahmed, S. F.; Poehlein, G. W. *Ind. Eng. Chem. Res.* **1997**, *36*, 2605–2615.
- (31) Le Bas, G. *The Molecular Volumes of Liquid Chemical Compounds*; Longmans Green: New York, 1915.
- (32) Hansen, F. K.; Ugelstad, J. In *Emulsion Polymerization*; Piirma, I., Ed.; Academic Press: New York, 1982; Chapter 2, pp 51–92.
- (33) Kawaguchi, S.; Winnik, M. A. *Macromolecules* **1995**, *28*, 1159–1166.

MA001690U